Available online at www.sciencedirect.com
ScienceDirect
Geochimica et Cosmochimica Acta 71 (2007) 2344–2360
Geochimica et Cosmochimica Acta
www.elsevier.com/locate/gca

Nitrogen concentration and $\delta^{15}N$ of altered oceanic crust obtained on ODP Legs 129 and 185: Insights into alteration-related nitrogen enrichment and the nitrogen subduction budget

Long Li *, Gray E. Bebout, Bruce D. Idleman

Earth and Environmental Sciences, 31 Williams Drive, Lehigh University Bethlehem, PA 18015, USA

Received 31 July 2006; accepted in revised form 1 February 2007; available online 6 February 2007

Abstract

Knowledge of the subduction input flux of nitrogen (N) in altered oceanic crust (AOC) is critical in any attempt to mass-balance N across arc-trench systems on a global or individual-margin basis. We have employed sealed-tube, carrier-gas-based methods to examine the N concentrations and isotopic compositions of AOC. Analyses of 53 AOC samples recovered on DSDP/ODP legs from the North and South Pacific, the North Atlantic, and the Antarctic oceans (with larger numbers of samples from Site 801 outboard of the Mariana trench and Site 1149 outboard of the Izu trench), and 14 composites for the AOC sections at Site 801, give N concentrations of 1.3 to 18.2 ppm and $\delta^{15}N_{Air}$ of $-11.6‰$ to $+8.3‰$, indicating significant N enrichment probably during the early stages of hydrothermal alteration of the oceanic basalts. The N–$\delta^{15}N$ modeling for samples from Sites 801 and 1149 ($n = 39$) shows that the secondary N may come from (1) the sedimentary N in the intercalated sediments and possibly overlying sediments via fluid-sediment/rock interaction, and (2) degassed mantle N_2 in seawater via alteration-related abiotic reduction processes. For all Site 801 samples, weak correlation of N and K_2O contents indicates that the siting of N in potassic alteration phases strongly depends on N availability and is possibly influenced by highly heterogeneous temperature and redox conditions during hydrothermal alteration.

The upper 470-m AOC recovered by ODP Legs 129 and 185 delivers approximately 8×10^5 g/km N annually into the Mariana margin. If the remaining less-altered oceanic crust (assuming 6.5 km, mostly dikes and gabbros) has MORB-like N of 1.5 ppm, the entire oceanic crust transfers 5.1×10^6 g/km N annually into that trench. This N input flux is twice as large as the annual N input of 2.5×10^6 g/km in seafloor sediments subducting into the same margin, demonstrating that the N input in oceanic crust, and its isotopic consequences, must be considered in any assessment of convergent margin N flux.
Published by Elsevier Ltd.

1. INTRODUCTION

Nitrogen (N) cycling between the surface and deep Earth, through constructive and destructive plate boundaries, determines the N signatures of Earth's major reservoirs (e.g., the atmosphere, crust, and mantle; Zhang and Zindler, 1993; Bebout, 1995; Javoy, 1998; Tolstikhin and Marty, 1998). It is necessary to compare subduction-zone input and output N fluxes in any effort to model geological N cycling and evaluate long-term evolution of the atmosphere and mantle (e.g., Fischer et al., 2002; Hilton et al., 2002; Sadofsky and Bebout, 2004; Li and Bebout, 2005). The geochemistry of N discharged by magmatism at mid-ocean ridges (MOR) and in volcanic arcs has been investigated in some detail, including work focused on several individual convergent margins that greatly improves our understanding of N return in arcs (e.g., Sano et al., 1998,

* Corresponding author. Present address: Equipe de Physico-Chimie des fluids géologiques, Institit de Physique du Globe de Paris, 2 Place Jussieu, tour 54-64 1er étage, 75251 Paris Cedex 05, France. Fax: +1 610 758 3677.
E-mail address: lol2@lehigh.edu (L. Li).

0016-7037/$ - see front matter Published by Elsevier Ltd.
doi:10.1016/j.gca.2007.02.001

2001; Fischer et al., 2002, 2005; Hilton et al., 2002; Snyder et al., 2003; Zimmer et al., 2004; Elkins et al., 2006). However, the N input flux in subducting lithologies has remained uncertain, and recent studies of N cycling based on volcanic gases have had to rely on estimates because of the lack of constraints on the N input inventory for the individual margins being investigated (Hilton et al., 2002; Fischer et al., 2002). Recent measurements of N concentrations and isotopic compositions of seafloor sediments from the Izu-Bonin-Mariana (IBM; Sadofsky and Bebout, 2004) and Central American margins (Li and Bebout, 2005) have provided better input fluxes for sedimentary N in these margins. However, the N subduction budget in AOC remains unknown (see discussion by Li and Bebout, 2005; cf. Scholl and von Huene, in press), limiting any attempts to compare subduction inputs and volcanic outputs for N.

Altered oceanic crust subducting into modern trenches is thought to play a key role in the crust-mantle cycling of many volatiles and mobile elements (Philippot et al., 1998; Alt and Teagle, 1999; Fischer et al., 2002; Hilton et al., 2002; Elliott, 2003; Jarrard, 2003). However, few studies have focused on the recycling of N in AOC into the mantle. Generally, fresh mid-ocean ridge basalts (MORB) contain very little N (mostly less than 2 ppm), reflecting the low N solubility in the upper mantle and related degassing of ascending magma beneath MOR (e.g., Cartigny et al., 2001). MORB samples show a wide range in $\delta^{15}N_{Air}$, which is defined as:

$$^{15}N = \frac{R_{sample} - R_{standard}}{R_{standard}} \times 1000 \quad (1)$$

where $R = \frac{^{15}N}{^{14}N}$ and the standard is atmospheric N_2. Most of the $\delta^{15}N$ values of MORB cluster around $-5 \pm 2‰$ after $^{40}Ar/^{36}Ar$-based corrections (Exley et al., 1987; Javoy and Pineau, 1991; Marty, 1995; Marty and Humbert, 1997; Sano et al., 1998; Marty and Zimmermann, 1999; Nishio et al., 1999). This $-5‰$ value is thought to represent the pristine N characteristics of the MORB source, a conclusion supported by $\delta^{15}N$ values of fibrous diamond (Javoy et al., 1984; Boyd et al., 1992; Cartigny et al., 2003). Between the time from their eruption at MOR to their subduction into trenches, oceanic basalts potentially undergo extensive water–rock interaction with seawater over a wide range of temperatures (Alt et al., 1986), perhaps even involving biogeochemical alteration (Bach and Edwards, 2003; Staudigel et al., 2006). These processes may significantly increase N contents of AOC by introducing secondary N components into the basalts. The secondary N is thought to be in form of NH_4^+ and located in the crystal lattice of K-rich clay minerals. This can occur because NH_4^+ is very similar to K^+ in its ionic radius and charge, and thus NH_4^+ can easily substitute for K^+ in these minerals (Yamamoto and Nakahira, 1966; Honma and Itihara, 1981; Bos et al., 1988). A recent examination of N in AOC at the East Pacific Rise (from ODP Leg 206) by Busigny et al. (2005a) yielded N concentrations mostly <10 ppm, far lower than those of seafloor sediments (hundreds to thousands of ppm; see Sadofsky and Bebout, 2004; Li and Bebout, 2005) but higher than those of MORB samples. However, Li and Bebout (2005) highlight that, because the volume of oceanic crust is far greater than that of the overlying sediments, the N subduction budget in oceanic crust could be comparable to that in sediments and must be considered in any attempt to mass-balance input and output N fluxes across subduction zones (also see Bebout, 1995; Hilton et al., 2002).

In this study, we employed sealed-tube, carrier-gas methods recently developed in our laboratory (Bebout et al., 2007) to investigate the N concentrations and isotopic compositions of AOC from the Pacific, Atlantic and Antarctic ocean basins recovered by DSDP/ODP drillings. We first present the results of a detailed study of AOC in the IBM margin (39 samples, including composites, from the sections drilled during Legs 129 and 185, at Sites 801 and 1149), with the goals of better defining the N input flux into the IBM convergent margin and identifying sources and mechanisms of N enrichment during seafloor alteration. We then present data for samples from various seafloor AOC sections (total of 14 samples) that help to constrain the range in N and $\delta^{15}N$ in the upper parts of other seafloor oceanic crustal sections.

2. GEOLOGICAL SETTING, SAMPLING, AND ALTERATION HISTORY

Two groups of samples were analyzed in this study. One group consists of 14 samples from DSDP Sites 279A, 319A, 332B, 396B, 417A/D, 448/448A, 458, 459B, 462A, and 504B (see Fig. 1a and Tables 1 and 2 for drilling locations). Previous studies show that the basalts from these sites experienced varying degrees of seafloor alteration, with the most intense alteration represented by AOC from Site 417 (Staudigel et al., 1996).

The other group consists of 39 AOC samples from Sites 801 and 1149 offshore of the Mariana and Izu-Bonin margins, respectively, and 14 composite samples for the basalt sections at Site 801 (see description and chemical analyses of these composites by Kelley et al. (2003)). The IBM margin is one of the reference sites for the MARGINS "Subduction Factory" initiative focusing on subduction-zone chemical cycling. The geological background of Sites 801 and 1149 and petrological and geochemical information regarding the AOC from those sites have been provided elsewhere (e.g., Plank et al., 2000; Alt and Teagle, 2003; Kelley et al., 2003), and are only briefly discussed here. The IBM system is formed by subduction of the Pacific plate beneath the Philippine plate. Site 801 is located in the Pigafetta Basin (the oldest part of the Pacific Ocean basin; ~170 Ma) outboard of the Mariana trench (Fig. 1b). Site 1149 is located ~100 km seaward of the Izu Trench, into which younger oceanic crust (~132 Ma) is being subducted (Fig. 1b). The subduction rate is very high (160 mm/yr) at Site 801 and considerably lower (51 mm/yr) at Site 1149 (Plank et al., 2000).

At Site 801, a total of 474 m (462–936 mbsf) of oceanic basalts were collected (133 m on Leg 129 in 1989 and 341 m on Leg 185 in 1999). This basalt section has been divided by lithology into eight major sequences (Plank et al., 2000; see Fig. 1b and c). From top to bottom, they are:

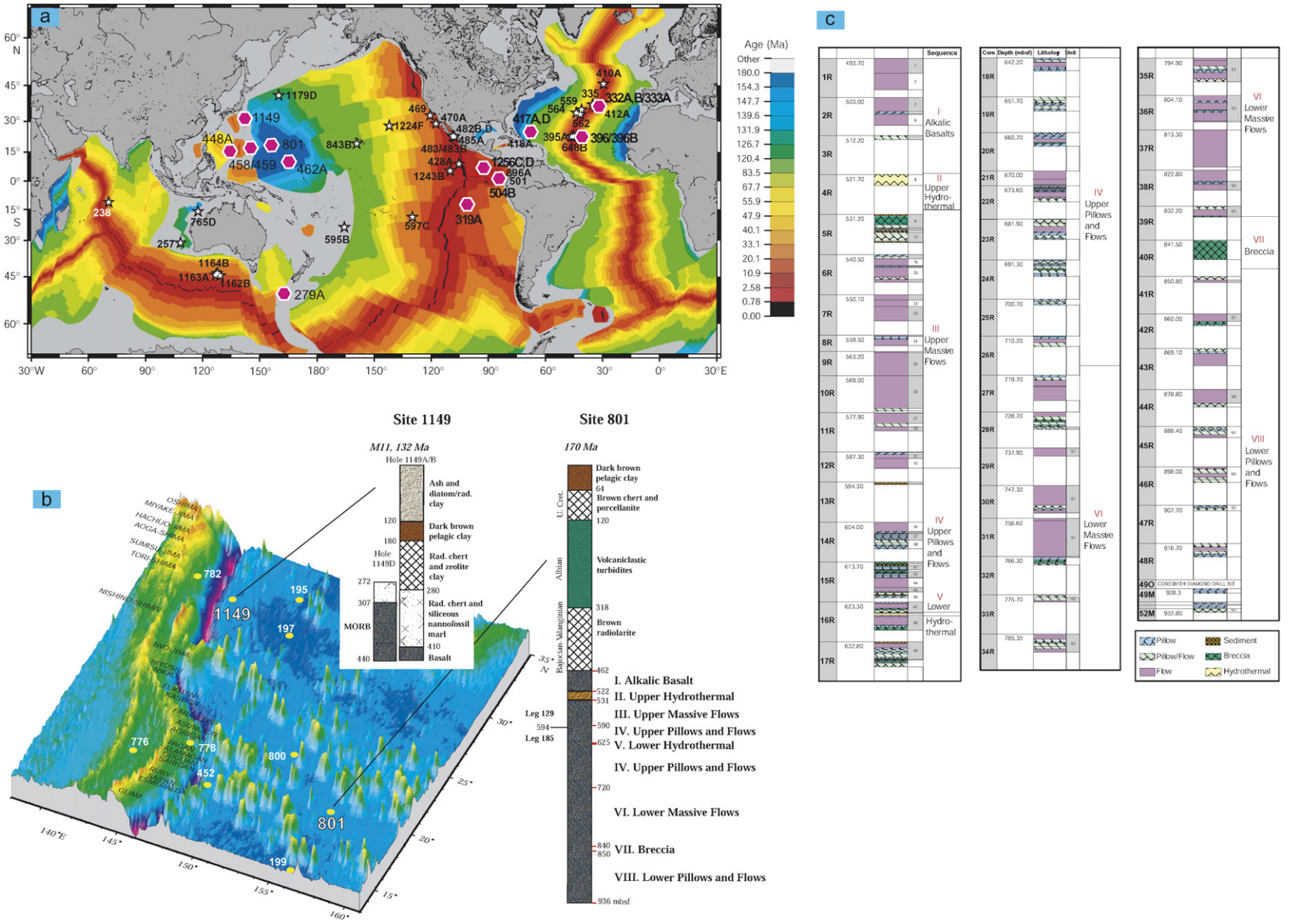

Fig. 1. (a) Map showing sites where oceanic crust samples have been recovered on DSDP/ODP legs (revised from Wilson et al., 2003). Filled hexagons represent sites from which basalt samples have been analyzed for N concentrations and isotopic compositions (Site 1256: Busigny et al., 2005; the other sites: this study; see Tables 1 and 2). Stars represent sites for which basalt N isotope analyses have not yet been undertaken. Age variations of the oceanic crusts are also shown. (b) Perspective map of Sites 801 and 1149 at the Izu-Bonin-Mariana convergent margin (revised from Plank et al., 2000). Note the lithologic variations of the oceanic crust recovered at Site 801. (c) Detailed lithologic information of oceanic crust at Site 801 drilled by Legs 129 and 185.

Table 1
Nitrogen concentrations and isotopic compositions of altered oceanic crust samples from Sites 801 and 1149 off the Izu-Bonin-Mariana trench

Location	Lithologic structure	Leg-Site	Sample number	Depth (mbsf)	Sample description[a]	N (ppm)	$\delta^{15}N_{Air}$ (‰)
Legs 129 and 185:Izu-Bonin-Mariana, Tropical Northwestern Pacific							
Lat.: 18°38.52′; Lon.: 156°21.582	I. Alkalic Basalts	129-801B	41R1 26–30	483.26	Slight to moderate alteration, a majority altered to green clay, some Fe stains around opaques	7.8	+0.7
		129-801B	43R1 22–27	492.42	Slight alteration, some green clays replacing non-pyroxene matrix, calcite-green clay veins present	9.5	0.2
		129-801B	43R1 132–135	493.52	Minimum alteration	2.8	−3.0
Lat.: 18°38.538′; Lon.: 156°21.588′		129-801C	1R1 109–141	494.79	Moderate alteration, white clay and smectite replacement, pyrite scattered throughout	7.5	−1.6
		129-801C	1R5 80–82	499.35	Moderate alteration with large carbonate vein	2.4	−4.9
	II. Upper Hydrothermal	129-801C	4R1 72–77	522.42	Hydrothermal deposit	3.0	0.0
	III. Upper Massive Flows	129-801C	5R2 12–17	532.58	Highly altered breccia with smectite-bearing vein network	13.4	+0.5
		129-801C	5R2 123–130	533.69	Highly altered breccia with large veins containing smectite and carbonate	17.1	+0.9
		129-801C	5R3 99–104	534.76	Highly altered pillow, glassy rims and ground mass altered to clay minerals, a few specks of pyrite present	16.3	+1.2
		129-801C	5R3 125–131	535.02	High alteration, devitrified rims and ground mass altered to green layers	15.3	+0.7
		129-801C	7R3 0–5	552.98	Slight alteration with smectite in vesicles and along veins	12.4	+0.1
		129-801C	8R1 18–21	559.68	Moderate to high alteration with clay and carbonate filled vesicles and replaced microlites	18.2	+0.7
		129-801C	8R1 65–67	560.15	High alteration with Fe-hydroxide stained margins	9.3	−0.2
		129-801C	10R6 67–70	576.83	Very slight alteration with green smectite replacing olivine and carbonate and/or clay filling vesicles and veins	6.7	+0.5
		129-801C	11R2 131–136	580.16	Slight to moderate alteration with replacement of mesostasis and microphenocrysts by green clays.	6.7	−0.1
		129-801C	12R1 101–104	588.31	Slight alteration with green smectite replacing glassy rims and olivine microphenocrsts, some green smectite oxidized with yellow coating	13.7	+1.0
		129-801C	12R3 57–62	590.83	Slight alteration with narrow halos	4.8	+0.9
	IV. Upper Pillows and Flows	185-801C	15R1 57–61	614.27	Red-yellow chert	1.5	−2.3
		185-801C	15R7 31–34	621.69	Sage, bleached basalt	3.4	−0.4
		185-801C	17R4 15–18	637.37	Green celadonite breccia cement, with small chunk of baked black basalt	3.0	−11.4
		185-801C	19R2 24–27	653.43	Hyaloclastite	1.8	−6.8
		185-801C	21R2 69–71	672.12	Massive calcite veins in aphyric basalts	2.8	−6.3
		185-801C	25R1 10–13	700.80	Minimally altered basalt	2.3	−7.0
	VI. Lower Massive Flows	185-801C	34R1 93–96	786.23	FeOx vein + halos in minimally altered basalt	1.3	−3.9
		185-801C	37R5 112–114	819.58	Fat smectite vein and large halos	2.5	−3.1
	VII. Breccia	185-801C	40R1 24–27	841.74	Brecciated basalt with calcite cement	3.6	−11.6

(*continued on next page*)

Table 1 (*continued*)

Location	Lithologic structure	Leg-Site	Sample number	Depth (mbsf)	Sample description[a]	N (ppm)	$\delta^{15}N_{Air}$ (‰)
	VIII. Lower Pillows and Flows	185-801C	43R1 13–15	869.23	Minimally altered basalt	3.8	−9.4
		185-801C	43R3 50–55	872.42	Huge celadonite vein with halos, not much basalt	2.3	−3.0
		185-801C	44R3 23–26	881.79	Calcite veins with halos	2.4	−5.9
		Composite-801[b]	TAB FLO	487.0		3.8	−7.9
		Composite-801	TAB VCL	487.0		6.0	−2.0
		Composite-801	TAB MIX	487.0		5.0	−2.5
		Composite-801	MORB 0–110 FLO	575.0		3.8	−6.2
		Composite-801	MORB 0–110 VCL	575.0		nd[c]	nd
		Composite-801	MORB 0–110 MIX	575.0		4.9	−7.1
		Composite-801	MORB 110–220 FLO	680.5		2.3	−4.1
		Composite-801	MORB 110–220 VCL	680.5		4.2	−9.4
		Composite-801	MORB 110–220 MIX	680.5		3.6	−6.2
		Composite-801	MORB 220–420 FLO	839.5		2.7	−5.0
		Composite-801	MORB 220–420 VCL	839.5		3.5	−10.2
		Composite-801	MORB 220–420 MIX	839.5		4.4	−6.6
		Composite-801	SUPER			3.9	−5.4
		Composite-801	SED			5.6	−0.5
Lat. 31°20.532′;	Pillow breccia	185-1149B	30R1 61–66	417.40	Breccia with big and little grey basalt clasts, calcite cement	1.4	−4.9
Lon.: 143°21.060′	Pillow	185-1149B	30R2 56–62	418.48	Well developed green halo in pink basalt with calcite vein	2.3	−1.8
Lat. 31°20.550′; Lon.: 143°21.060′	Pillow	185-1149C	10R2 47–51	409.39	Grey basalt, minimally altered	2.7	−2.8
Lat. 31°18.792′;	Breccia	185-1149D	7R1 37–42	320.09	Hyaloclastite, many small fragments, greenish grey	2.5	−0.8
Lon.: 143°24.024′	Pillow/flow	185-1149D	9R3 30–32	341.79	Pink basalt with orange, green, brown halos	2.1	−7.9
	Flow	185-1149D	11R2 86–92	360.13	Breccia, dark-grey basalt clasts in calcite matrix	1.5	−6.9
	Pillow/flow	185-1149D	16R3 2–8	408.93	Grey basalt, minimally altered	1.7	−6.5
	Breccia	185-1149D	17R1 92–98	416.45	Dark grey basalt, some calcite veins	1.4	−4.3
	Pillow	185-1149D	19R1 85–89	435.57	Dark grey basalt, minimally altered	2.5	−10.5

[a] Samples description was provided by Lancelot et al. (1990) and Kelley (person. commun.).

[b] The basement at Site 801 is divided into 4 intervals (the alkaline basalt sills and 3 MORB sections) according to the geochemical characterization of more than 100 communal samples (Plank et al., 2000). For each interval, one composite was made for submarine extrusives (FLO) and clastic rocks (VCL) by combing proportional communal samples. FLO and VCL are then combined into the MIX composite in a ratio of 30–70%. The SUPER composite was made for the entire MORB interval by combing the 3 MORB composites. The SED composite was made for the intercalated sediments in the upper 230 m of the basement (mostly in Sequences I, III, and IV, see descriptions by Plank et al., 2000; Alt, 2003).

[c] No data.

Table 2
Nitrogen concentrations and isotopic compositions of a 14-sample survey on AOC recovered by DSDP drillings from the Antarctic, Atlantic, and Pacific

Location	Leg-Site	Sample number	N (ppm)	$\delta^{15}N_{Air}$ (‰)
Tasman ridge, Antarctic (Lat.: −51.3357°; Lon.: 162.6350°)	29-279A	13R2 0–2	3.3	+0.5
	29-279A	13R2 116–120	4.7	+4.2
South Pacific (Lat.: −13.0173°; Lon.: −101.5243°)	34-319A	3R4 50–53	2.6	+0.1
North Atlantic (Lat.: 36.8787°; Lon.: −33.6410°)	37-332B	33R2 77–80	7.8	−5.4
North Atlantic (Lat.: 22.9857°; Lon.: −43.5150°)	46-396B	15R3 83–89	12.1	+4.8
North Atlantic (Lat.: 25.1105°; Lon.: −68.0413°)	51-417A	38R8 Alt	14.6	+0.6
	51-417A	44R4 Alt	11.9	+8.3
North Atlantic (Lat.: 25.1115°; Lon.: −68.0468°)	51-417D	33R5 Alt	10.6	+4.0
Philippine Sea (Lat.: 16.3410°; Lon.: 134.8742°)	59-448A	41R1 2–7	6.5	+3.3
	59-448	61	11.7	+3.8
North Pacific (Lat.: 17.8642°; Lon.: 146.9343°)	60-458	33R2 74–77	13.4	+5.5
North Pacific (Lat.: 17.8625°; Lon.: 147.3015°)	60-459B	66R1 100–102	15.2	+6.2
North Pacific (Lat.: 7.2417°; Lon.: 165.0317°)	61-462A	22R2 120–124	7.6	−0.6
Central Pacific (Lat.: 1.2272°; Lon.: −83.7302°)	70-504B	35R1 10–15	3.6	−5.1

(I) Alkali Basalts: thick unit of alkaline basaltic to doleritic sills (Floyd et al., 1992), intercalated with some chert-rich sediments baked by basalts at contacts (462–522 mbsf);
(II) Upper Hydrothermal: highly permeable Si- and Fe-oxyhydroxide-rich hydrothermal unit (10–20 m thick);
(III) Upper Massive Flows: massive MORB tholeiitic flow showing varying intensities of alteration from 531 to 590 mbsf (recrystallized sediment layers in thickness of cm to dm are common in Sequences III and IV);
(IV) Upper Pillows and Flows: pillows and flows with well-developed interpillow horizons (590–720 mbsf);
(V) Lower Hydrothermal: ocherous, Fe–Si-rich, low-temperature (*T*) hydrothermal zone (~1 m thick) at 625 mbsf;
(VI) Lower Massive Flows: 720–840 mbsf, including some pillows as thick as 15 m with a well-defined rubbly base;
(VII) Breccia: 840–850 mbsf; and
(VIII) Lower Pillows and Flows: >850 mbsf.

According to Ar geochronology, Pringle (1992) suggested that there is an interval of 5–15 Myr between the intrusion of the alkaline sill (Sequence I) and the initial accretion of the tholeiitic crust (Sequence III–VIII), which is divided by the Upper Hydrothermal deposits (Sequence II). However, more recent studies (Koppers et al., 2003; Pockalny and Larson, 2003) reinvestigated the basalt sections at Site 801 and divided them into an earlier-emplaced "lower series" (Sequences IV–VIII; >168 Ma) and a later-erupted "upper series" (Sequences I–IV; ~160 Ma), which is defined by the Lower Hydrothermal deposits (Sequence V) within Sequence IV. Those studies confirmed that there is a 10-Myr gap between the "lower series" and the "upper series".

During Leg 185, a total of 196 m of basement were recovered from Sites 1149 B, C, and D with the best recovery of 130 m of the igneous units at Site 1149D (Plank et al., 2000). The rocks recovered at these sites are mostly pillows or thick flows, including some interpillow breccia, similar to Sequence IV at Site 801 (Plank et al., 2000).

The AOC at Site 801 are primarily aphyric to slightly phyric plagioclase- and/or olivine-bearing basalts, containing two large Fe-oxyhydroxide hydrothermal deposits. Aphyric pillow basalt is the dominant lithology at Site 1149. The groundmass of the basalt is mainly composed of euhedral plagioclase, euhedral to subhedral pyroxene and olivine, dispersed euhedral oxides, and interstitial cryptocrystalline and brownish devitrified glass. Detailed summaries of alteration type and fluid evolution were presented by Alt et al. (1992), Plank et al. (2000), and Alt and Teagle (2003). Generally, the alteration of basalts at Site 801 can be divided into at least three categories (Alt et al., 1992; Plank et al., 2000; Alt and Teagle, 2003):

(1) Dark-grey alteration. All of the rocks from Site 801 experienced pervasive but minor background dark-grey alteration. In this type of alteration, all olivine and the interstitial glass in the groundmass have been replaced by smectite, but most plagioclase phenocryst/microlite and intergranular augite are left unaltered. Secondary replacement minerals (30–80 vol% in Sequence I and 2–20 vol% in the lower tholeiitic sequences) include saponite and calcite filling in the veins and pore spaces and common disseminated pyrite (Alt et al., 1992; Plank et al., 2000; Alt and Teagle, 2003). The intensity of dark-grey alteration at Site 801 is greater in the upper part of the core (i.e., Sequences I and III) and decreases downward (Plank et al., 2000; Alt and Teagle, 2003), as has been observed in other cores (e.g., Staudigel et al., 1995; Alt et al., 1996). The occurrence of dark alteration halos (1–18 mm wide) along veins in the tholeiitic rocks is common. These halos are characterized by celadonite and Fe-oxyhydroxides replacing olivine and are interpreted as having formed at the early stage of vein-related alteration from the upwelling distal hydrothermal fluids (Alt and Teagle, 2003).

(2) Brown alteration. Brown alteration is similar to the dark-grey background alteration but characterized by the presence of abundant Fe-oxyhydroxide finely disseminated in the ground mass, reflecting greater fluxes of oxygenated seawater than in the dark-grey, pyrite-bearing rocks (Alt et al., 1992; Plank et al., 2000; Alt and Teagle, 2003). Celadonite may be present as a result of the superposition of brown and dark alteration halos. The brown halos are only 2 vol % and limited to above 150 m and below 300 m in the core (Alt and Teagle, 2003).
(3) Green-buff alteration. This alteration type occurs in basalts beneath the hydrothermal deposits, probably related to the upwelling hydrothermal fluids that formed the deposits. The green-buff alteration involved intense replacement (80–100 vol% for green type and 60–80 vol% for buff type) of the rare olivine and plagioclase phenocrysts, the microlites, and the ground-mass by celadonite, glauconite, smectite (beidellite–montmorillonite), K-feldspar, calcite and titanite (Alt et al., 1992; Plank et al., 2000; Alt and Teagle, 2003).

Based on oxygen-isotope thermometer, Alt and Teagle (2003) provide estimated formation temperatures of 35–95 °C, generally increasing downward, for secondary quartz, saponite, celadonite, and smectite. Temperatures estimated for carbonate veins range to lower temperatures, ~15–65 °C, also generally increasing downward.

The altered basalts at Site 801 show obvious chemical changes as a result of low-T water–rock interaction and consequent formation of secondary minerals, including loss of Mg, Mn, Ni, Zn, Cu and gain of K_2O, Ce, Ba, Rb, H_2O and CO_2. This effect is greatest in green-buff rocks and smallest in dark-grey rocks (Alt and Teagle, 2003). Iron in altered basalts is either depleted or enriched, depending on whether the alteration resulted in the breakdown of titanomagetite or the deposition of Fe-oxyhydroxide (Alt et al., 1992; Plank et al., 2000; Alt and Teagle, 2003).

The basalts from Site 1149 were pervasively and strongly altered (mostly dark-grey type) by oxidizing water–rock interactions, producing abundant veins including Fe-oxyhydroxide deposits, alteration halos, and breccias (Plank et al., 2000). The alteration history at Site 1149 occurred in three stages (Plank et al., 2000):

(1) Early fracturing of basalt with filling of veins by clay minerals (mostly saponite) and development of celadonitic phyllosilicates in cracks, vesicles, miarolitic voids, and as a replacement of the olivine and mesostasis.
(2) Progressive alteration and oxidation of phyllosilicates or addition of Fe oxide, to these zones to produce goethite and/or mixtures of clay mineral + goethite (i.e., "iddingsite"). The fluids responsible for this alteration stage followed the same pathways as those of the first stage, as well as in new hairline cracks, resulting in the development of brown oxidation halos near fractures.
(3) Reopening of veins allowing the circulation of fluids with evolved compositions and precipitation of carbonate and further alteration on previous halos.

3. ANALYTICAL METHODS

In this study, we employed sealed-tube, carrier-gas methods developed in our laboratory for analyses of low-N silicate materials (methods described in Bebout et al., 2004, 2007). For most of the AOC samples, 50–350 mg powder (depending on the N content) was loaded with Cu_xO_x reagent into quartz tube (outer diameter: 6 mm; inner diameter: 4 mm) and pumped for 48 h while heated to temperatures of ~100 °C. The 400–450 °C precombustion/oxidation step used by Busigny et al. (2005b) and Ader et al. (2006) for removal of modern organic contamination was not employed in this study in order to avoid N degassing of clay minerals and the removal of any possible organic matter that was present in these rocks on the seafloor (e.g., attributable to microbial alterations; see Staudigel et al., 2006). After the pumping and initial low-T heating step, the tubes were sealed under high vacuum and combusted at 950 °C for 3 h in a programmable furnace. The N_2 produced by the combustion was purified using a liquid nitrogen trap and introduced, in a helium stream, into a Finnigan MAT 252 mass spectrometer. A gas chromatographic column in the Finnigan Gas Bench II system we employ separates N_2 from other gases such as CO (interference on m/z 28 and 29). Nitrogen concentration was determined by interpolating measured N peak area to a calibrated relationship between N peak area and N concentration. Uncertainty (expressed as 1σ for $\geqslant 3$ replicate analyses of both internal silicate standards and individual AOC samples) is less than 5% for N concentration and on the order of 0.15‰ for $\delta^{15}N$. However, uncertainty in $\delta^{15}N$ increases to about 0.6‰ for N size less than 40 nmol. Thus, large sample sizes (500–1000 mg) were used for samples containing only 1–2 ppm N in order to maintain high precision for all analyses. Total system blanks depend largely on the amounts of reagent used, but the blanks are uniform in size and isotopic composition for certain amount of reagent, allowing accurate corrections to be performed on data for unknowns (Bebout et al., 2004, 2007). For example, in a 2-month period, 29 analyses of the system blank using 1 g Cu_xO_x reagent indicate an average blank size of 3.8 ± 0.2 nmol N_2, with $\delta^{15}N$ of -7.3 ± 0.4‰.

We conducted a number of tests aimed at evaluating the yields (as a function of temperature and duration of combustion), precision of the analyses, and the extent of any contributions of adsorbed atmospheric N_2. Experiments on one AOC sample from Site 504B produced similar yields (nmoles N_2/gram sample) and isotopic compositions when combusted at 950, 1000, and 1050 °C (Fig. 2), indicating that heating to 950 °C is sufficient for quantitative extraction of N from these samples. Heating to 950 °C is also employed in another recent study of N in AOC (Busigny et al., 2005b). For 10 AOC samples, we recombusted the residues for 3 h at 1000 °C two weeks after their first combustion at 950 °C. These recombustions produced blank-level

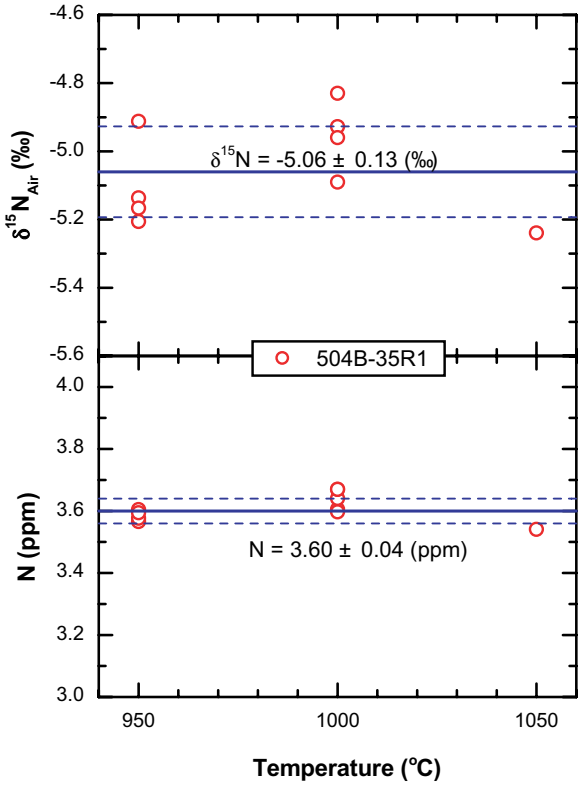

Fig. 2. Nitrogen concentration and isotopic composition of 504B-35R1 obtained by combustions at different temperatures. Aliquots of AOC sample 504B-35R1 were combusted at 950°, 1000°, and 1050 °C to identify the best experimental conditions. The results show similar values in N concentration and isotopic composition for this sample at all temperatures, indicating that combustion at 950° is sufficient for complete N extraction.

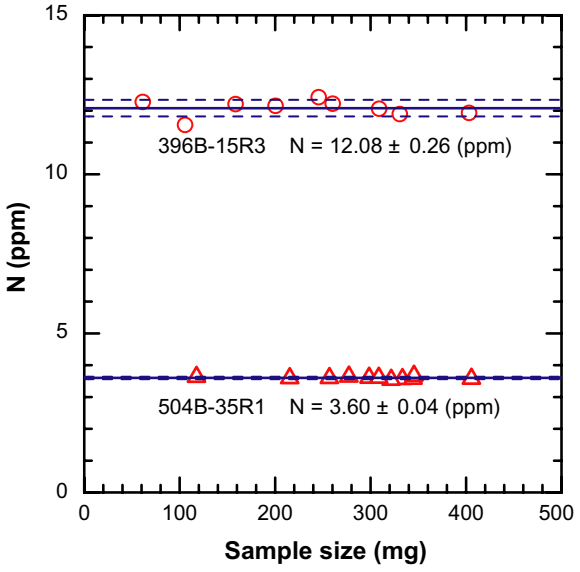

Fig. 3. Nitrogen concentrations measured for 504B-35R1 and 396B-15R3 over a wide range of sample sizes. This experiment is designed to examine the possible atmospheric absorption effect on the powder surface, and as an overall test of the reproducibility of the analyses of N concentration. The range from 50 to 400 mg covers the variation in sizes we used for most other analyses in this study.

amounts of N_2, again demonstrating complete N yields by heating to 950 °C and also implying that the contamination by (air-borne) modern organisms (e.g., bacteria, pollen) is probably not significant. As another demonstration of the consistency in yields, analyses of two AOC samples showed no differences in N concentrations over a sample size range of 50 mg to >400 mg (Fig. 3), which covers the range of sample sizes on which we performed extractions for most of the other AOC. For this series of analyses (Fig. 3), the precision (again, as 1σ) of the analyses of N concentration and $\delta^{15}N$ are 2% and 0.15‰, respectively.

4. RESULTS

The N concentrations and isotopic compositions of AOC obtained in this study are provided in Table 1 for Sites 801 and 1149 and Table 2 for the other sites. Altered oceanic basalts from Site 801 show a large variation in both N concentration (from 1.3 to 18.1 ppm) and $\delta^{15}N$ (from −11.6‰ to +1.2‰; Table 1). The highest N concentrations and $\delta^{15}N$ values occur in the "upper series" (corresponding to Sequences I and III in this study considering that only one sample from the upper part of Sequence IV is measured) at Site 801 (Figs. 4 and 5). Moreover, relatively high N concentrations are associated with high $\delta^{15}N$ values and relatively low N concentrations are mostly associated with extremely low $\delta^{15}N$ values (Figs. 5 and 6). As expected, the composites of AOC from Site 801 (Kelley et al., 2003) have intermediate N concentrations of 2.3 to 6.0 ppm and $\delta^{15}N$ of −0.5‰ to −10.2‰ (Table 1). These values are consistent with the averages of the AOC samples for all of the sequences but MORB 0–110 (corresponding to Sequences III and IV). Because of the limit of sample size, no duplicate analyses can be carried out for composites. Thus, it is unclear whether this discrepancy for MORB 0–110 is caused by composite preparation or the isotope determination. Nine AOC samples from Site 1149 show relatively low N concentrations of 1.4 to 2.7 ppm with $\delta^{15}N$ of −10.5‰ to −0.8‰. The samples from the upper part of the basement at Site 1149 contain somewhat higher N with higher $\delta^{15}N$ values (Table 1; Fig. 6). However, the N enrichment in this section is not as striking as that at Site 801. Fourteen AOC samples from the Pacific, Atlantic and Antarctic oceans (also see Table 2 for detailed localities) show a range in N concentration similar to that for Site 801, from 2.6 to 15.2 ppm, but with higher $\delta^{15}N$ values ranging from −5.4‰ to +8.3‰. Combining the data for all of the sites (using weight averaged data for Sites 801 and 1149), a crude positive linear relationship ($R = 0.66$) is observed between N concentrations and $\delta^{15}N$ values (Fig. 7).

5. DISCUSSION

5.1. Hydrothermal alteration and N enrichment

Most of the AOC samples analyzed in this study (Tables 1 and 2) have N concentrations higher than those of

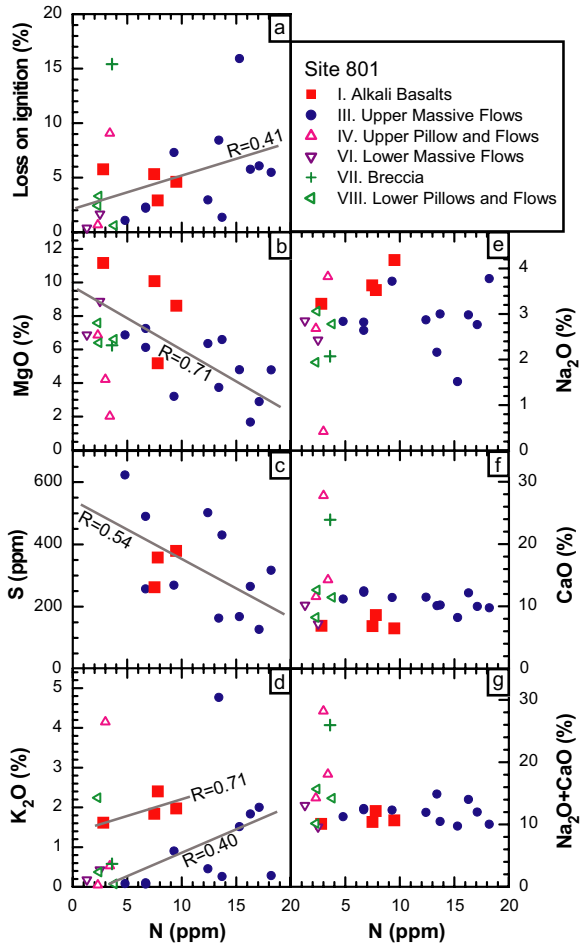

Fig. 4. Plots of concentrations of N and other elements for basalt samples from Site 801. (a) Loss on ignition (LOI). (b) MgO. (c) S. (d) K_2O. (e) Na_2O. (f) CaO. (g) $Na_2O + CaO$. No clear relationship appears for Sequences IV–VIII. The correlations of N with LOI, MgO, and S indicate the key role of hydrothermal alteration for N enrichment. Weak relationship between N and K_2O (particularly in Sequence III) reflects heterogeneity in N availability and possibly also in alteration conditions (e.g., temperature, redox). The absence of correlations of N with Na_2O and CaO indicate Na- and Ca-rich phases are not important sites for N residence.

MORB, with the latter generally containing less than 2 ppm N, reflecting significant N enrichment in these AOC samples. Where and how this N can reside in AOC are not well constrained but have to be answered for the understanding of processes controlling N cycling in seafloor environments. Recent study of AOC from ODP Site 1256, in the east Flank of the East Pacific Rise (Busigny et al., 2005a), has excluded salts (e.g., NH_4Cl and $[NH_4]_2SO_4$) as hosts of the enriched N, based on comparison of N data for samples with and without acid rinsing treatments. For Site 801, textures and geochemical properties of the basalts imply that microbial activity exists but is minor in these rocks (Fisk et al., 1999). In addition, characteristic C-isotope fractionation during biological processes may produce extremely low $\delta^{13}C$ of carbonate ($-23‰$ to $-3‰$; see Staudigel et al., 2006 and references therein), which is not detected from Site 801 samples (Alt and Teagle, 2003). Thus, the contribution of N by microbial biomass to those rocks may be negligible. Based on these observations, we assume that the secondary N occurs largely in the form of ammonium (NH_4^+) in mineral lattices substituting for K^+. Busigny et al. (2005a) also suggested that Na and Ca sites in plagioclase could be potential sites for secondary N.

In an attempt to test these assumptions and further evaluate the mechanisms by which N was sequestered in the AOC from Site 801, we examined the possible concentration correlations between N and other major and trace elements in the altered basalts (see data in Castillo et al., 1992 and Kelley et al., 2003; original concentration data for major elements and sulfur of Site 801 samples are also listed in Table 3). For the "lower series", no clear correlation was observed between N and any other element (Fig. 4), probably because limited availability of N influenced the extents of N incorporation (see the discussion below). For the "upper series", N concentrations positively correlate with LOI contents (Fig. 4a) and negatively correlate with MgO and S concentrations (Fig. 4b and c). No correlations were observed in the "upper series" between N and other major and trace elements, including those geochemically similar to N and K (e.g., Rb). In general, increase in LOI content of oceanic basalt can be attributed to alteration-induced transformation of primary phases and glass to hydrated phases (Plank et al., 2000). Alteration can also lead to S loss from basalt due to the loss of igneous sulfide minerals (e.g., Hart et al., 1974; Plank et al., 2000). But alteration generally results in Mg gain due to the formation of secondary Mg-bearing minerals (e.g., smectite, tremolite–actinotite, talc; Hart et al., 1974; Mottl and Holland, 1978). In contrast with the observation at other sites and even for the "lower series" at Site 801, Mg loss occurred in the "upper series" because of the intense low-T hydrothermal alteration (green-buff type) that induced extensive breakdown of olivine (e.g., Plank et al., 2000; Alt and Teagle, 2003). Therefore, the relationships in Fig. 4a–c consistently show the key role of hydrothermal alteration in the incorporation of secondary N into AOC. The covariation of N enrichment with degrees of alteration and the formation of secondary hydroxyl-bearing minerals (Figs. 4a–c and 5a) demonstrates that the secondary clay minerals are the most likely hosts for the enriched N. Based on the observations that an obvious relationship between the concentrations of N and Na or Ca (or the sum of both concentrations; Fig. 4e–g) is lacking and that high N concentrations with high $\delta^{15}N$ values tend to be in the high-K zones (Fig. 5b–d), K^+, rather than Na^+ and Ca^{2+}, is believed to be the site housing secondary N. In fact, four AOC samples from Sequence I show a relatively strong linear relationship between N and K_2O concentrations ($R = 0.71$; see Fig. 4d), whereas ten AOC samples from Sequence III define a relatively poor relationship ($R = 0.40$), reflecting the complexity of the siting of secondary N controlled by other factors.

The major factor other than alteration that may affect N incorporation of AOC is the availability of secondary N. In general, clay minerals are capable of incorporating large amounts of N, and hundreds to thousands of ppm N have been observed in clay fractions of both sedimentary rocks

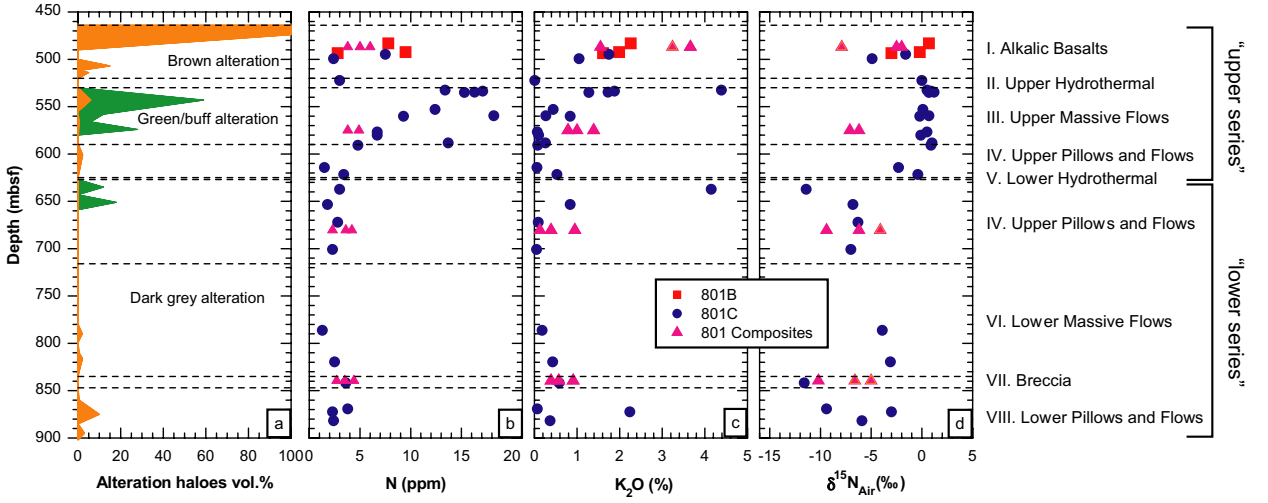

Fig. 5. Downhole variation of hydrothermal alteration, N concentration, K_2O concentration, and $\delta^{15}N$ of samples and composites from Site 801. (a) Volume percentage of brown (in brown/light grey), green/buff (in green/dark grey) and dark-grey (in white) alteration (from Alt and Teagle, 2003). (b) N concentration. (c) K_2O concentration (data from Castillo et al., 1992; Kelley et al., 2003). (d) $\delta^{15}N$ value. Most high-N bearing samples are from Sequences I and III, which are also intensely altered zones. K_2O enrichment is also observed in these two zones. However, N concentration is not strictly correlated with K_2O concentration on an individual-sample basis (Fig. 4d), perhaps due to the heterogeneities in N availability and local temperature and redox conditions during alteration (see text for discussion).

(e.g., Williams et al., 1995; Schroeder and McLain, 1998) and altered oceanic basalts (Busigny et al., 2005a). However, whether clay minerals can sequestrate a significant amount of N strongly depends on the availability of secondary N and how efficiently it is supplied. When the "lower series" basalts were formed, sediments were likely scarce to absent as no intercalated sediments were observed in this section (Plank et al., 2000). In such cases, the N available to AOC is the limited dissolved inorganic N (DIN) in seawater. At MOR, one of the major components of DIN is N_2 degassed from ascending magmas (see the discussion in 5.2). This N could have migrated into the basalts in upwelling hydrothermal fluids. When the degassed mantle N_2 and alteration-liberated basaltic N_2 (i.e., as inclusions in basaltic minerals) reacted with the H_2 produced by low-T alteration of basaltic minerals (mostly olivine and pyroxene; Stevens and McKinley, 2000), the Haber process ($N_2 + 3H_2 \rightarrow 2NH_3$) could have been driven to produce ammonia (NH_3) under reducing conditions thought to have existed at a variety of alteration stages from the formation of alteration halos in the early stages to the deposition of carbonate veins in the late stages at Site 801 (Alt and Teagle, 2003). The pyrite formed during the alteration of those basalts (Plank et al., 2000; Alt and Teagle, 2003) could have significantly promoted the synthesis of NH_3/NH_4^+ (Schoonen and Xu, 2001). The supply of NH_3/NH_4^+ to AOC by the Haber process is believed to be slow and less efficient, but the sequestration of measurable amounts of N produced by this process is still possible. For the "upper series", on the other hand, a significant sediment reservoir (as thick as 15–45 m after accumulation for 5–15 Myr at an overall depositional rate of ~3 m/Myr for Site 801; Lancelot et al., 1990) could have existed before the basalts formed and subsequently been intercalated when the basalts were emplaced. Circulation of hydrothermal fluids induced by the magmatic intrusion could have leached NH_4^+ from intercalated sediments, and the overlying sediments (if present). This NH_4^+ could then have been fixed into secondary clay minerals. A similar process appears to be operating at the "unsedimented" Endeavour segment of the Juan de Fuca Ridge, where anomalously high concentrations of NH_4^+ and CH_4 characterized by organic $\delta^{13}C$ have been observed in hydrothermal fluids and attributed to the decomposition of organic matter in previously deposited, now-buried sediments (Lilley et al., 1993; Proskurowski et al., 2004). Although the abiotic reduction process could also possibly occur in the "upper series", any effect of this kind of N must have been overwhelmed by the dominant incorporation of sedimentary N. Because of different N availabilities, the "lower series" basalts are characterized by low N concentrations and low $\delta^{15}N$ values, whereas the "upper series" basalts are characterized by high N concentrations and high $\delta^{15}N$ values (Fig. 5). Among the "upper series", Sequence I is less enriched in N than Sequence III. Two factors may be responsible for this observation: (1) the available sedimentary N decreased with the decomposition of sedimentary organic matter when Sequence I was emplaced; (2) Sequence I is characterized by oxygenated seawater alteration (brown type), whereas Sequence III is characterized by relatively reduced fluid alteration (green-buff type), which favors the incorporation of NH_4^+.

Some other important factors that can affect N incorporation of AOC may be related to the geochemical conditions during the hydrothermal alteration. Assuming a relatively large N reservoir during the alteration of the "upper series" at Site 801, the highly variable N concentrations in a single sequence (i.e., I or III) should be attributed to the heterogeneities in alteration intensity and local temperature and redox conditions (on the scale of centimeters;

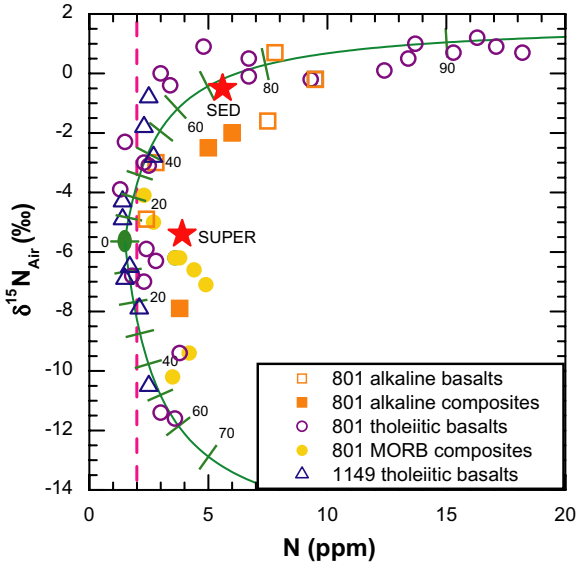

Fig. 6. Diagram of N concentrations and isotopic compositions for individual AOC samples from Sites 801 and 1149 and for composites for Site 801. Note that (1) samples with less than 2 ppm N (mean 1.5 ppm) and $\delta^{15}N$ values around −5.6‰ may represent characteristics of "fresh" basalts; (2) high N-bearing samples (>4 ppm) have relatively homogeneous $\delta^{15}N$ values around $+0.4 \pm 0.7$‰, implying that the most significant enrichment of N is from sediments; (3) the N with extremely negative values could possibly be attributed to abiotic reduction of mantle-like N_2 to NH_3 and then assimilation of this NH_3/NH_4^+ by AOC (see text for discussion). Also shown are two-endmember mixing lines between MORB and sedimentary N (upper line) and between MORB and abiotically reduced N (lower line). Numbers along the mixing lines represent fractions of secondary N from corresponding source. Nitrogen compositions for the three endmembers are: (1), "Fresh" MORB: $N = 1.5$ ppm and $\delta^{15}N = -5.6$‰, based on the data average of six relatively unaltered basalts from Sites 801 and 1149. (2) Sediments: $\delta^{15}N = +1.8$‰, based on the data average of the lowest overlying sediment samples analyzed at 801 (Sadofsky and Bebout, 2004) and the composite of intercalated sediments in basalts. (3) NH_3 reduced from mantle-like N_2: $\delta^{15}N = -16$‰, based on a N-isotope fractionation of 11‰ at the hydrothermal temperatures (Urey, 1947; Hanschmann, 1981). In these calculations, poorly known N isotope discrimination is neglected for the other steps of N transfer that involve no species change of N.

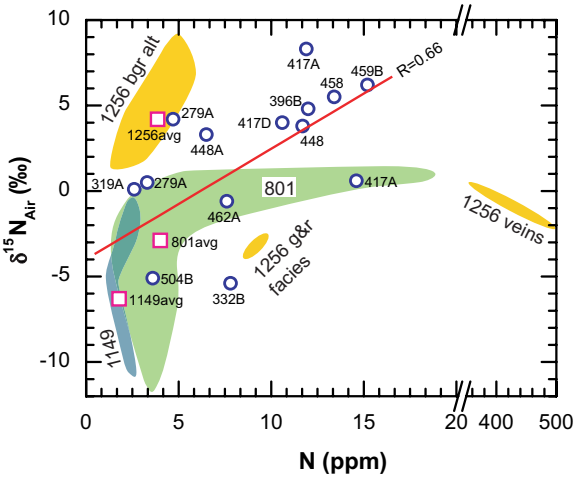

Fig. 7. Diagram of N concentrations and isotope compositions for 14 AOC samples (circles) from the Atlantic, Pacific, and Antarctic. The data ranges (shadow) and averages (squares) for Sites 801 and 1149 (this study), and 1256 (bgr alt: background alteration; g&r facies: green and red facies; Busigny et al., 2005a) are also shown. A positive trend between N concentrations and isotopic compositions apparently reflects extensive incorporation of sedimentary N into these AOC, but the correlation ($R = 0.66$) is weakened by localized differences in N source compositions, N availability, and alteration conditions (e.g., temperature and redox). These factors may vary significantly even in the same site, as reflected by the data for Sites 417, 801, 1149, and 1256.

Alt and Teagle, 2003). The variation of these parameters could directly influence the efficiency of N incorporation, resulting in the heterogeneous distribution of N concentrations (Figs. 4 and 5) and yielding the poor relationship between N and K_2O concentrations for Sequence III (Fig. 4d).

The more "global" comparison also points to widely varying degrees of N enrichment in AOC (Fig. 7). Because the samples are all from the topmost part of the basement at sites other than 801 and 1149, they had the best chance to obtain sedimentary N once the overlying sediments accumulated. Therefore, the correlation between N concentration and $\delta^{15}N$ ($R = 0.66$; Fig. 7) may reflect large-scale variation in N availability, isotopic compositions of sedimentary sources, temperature, and the redox conditions of the hydrothermal alteration.

5.2. Nitrogen sources

The sources of secondary N can be inferred from the combined N concentration and isotopic data because the potential sources (mantle, seawater DIN, and seafloor sediments) are quite distinct in their $\delta^{15}N$ values and the isotope fractionations related to change in N speciation are high at the temperatures of the alteration. Among the major N reservoirs, seafloor sediments show relatively high $\delta^{15}N$ values, varying from −0.9‰ to +5.0‰ in the Mariana margin and +2.5‰ to +8.2‰ in the Izu margin (Sadofsky and Bebout, 2004); seawater DIN in benthic environment around MOR includes minor NH_4^+ and some N_2 from the outgassing of ascending magma. As the product of complete reduction of NO_3^-, NH_4^+ should inherit the high $\delta^{15}N$ of NO_3^- (0–12‰, Cline and Kaplan, 1975; Brandes et al., 1998). Degassed N_2 from the mantle should have mantle-like $\delta^{15}N$ values, possibly with a negative shift of 1–2‰ as a result of degassing-related isotope fractionation (Cartigny et al., 2001).

At Sites 801 and 1149, AOC can be divided into three groups based on their N concentrations and isotopic compositions: (1) samples containing less than 2 ppm N (except a chert sample 801C-15R1; averages are 1.5 ± 0.2 ppm N with $\delta^{15}N$ values of -5.6 ± 1.3‰ for six AOC samples), (2) samples containing more than 4 ppm N (all from Sequences I and III at Site 801) with relatively homogeneous $\delta^{15}N$ values around $+0.4 \pm 0.7$‰, and (3) samples

Table 3
Major element and sulfur concentrations of AOC samples employed in this study from Site 801

Leg-Site	Sample number	SiO_2	TiO_2	Al_2O_3	Fe_2O_3[a]	FeO	MnO	MgO	CaO	Na_2O	K_2O	P_2O_5	Total	LOI	S (ppm)	Note
129-801B	41R1 26–31	45.77	3.31	16.03	4.76	4.72	0.14	5.2	8.25	3.81	2.14	0.62	99.8	5.09	358	c
129-801B	43R1 22–27	45.88	2.94	15.23	4.70	5.70	0.13	8.28	6.21	4.02	1.90	0.55	100.1	4.58	379	c
129-801B	43R1 132–135	47.30	2.42	13.54	12.51	nd[b]	0.153	11.16	6.85	3.22	1.61	0.512	99.28	5.74	nd	d
129-801C	1R1 109–141	44.92	2.80	14.72	3.62	6.4	0.15	9.58	6.46	3.45	1.75	0.60	99.8	5.30	263	c
129-801C	1R5 80–82	20.12	1.12	6.91	19.53	nd	0.863	24.43	23.70	1.60	1.05	0.290	99.62	34.29	nd	d
129-801C	4R1 72–77	85.63	0	0.58	12.78	nd	0.0112	0.0614	0.0275	0.119	0.0122	0.0179	99.24	1.90	nd	d
129-801C	5R2 12–17	48.10	1.02	15.75	6.49	1.29	0.18	3.44	9.31	1.99	4.39	0.01	100.4	8.43	163	c
129-801C	5R2 123–130	50.75	1.03	17.89	4.91	2.44	0.09	2.72	9.38	2.60	1.88	0.02	99.8	6.08	127	c
129-801C	5R3 99–104	51.59	1.16	19.76	1.97	1.90	0.11	1.58	11.48	2.81	1.73	0.01	99.9	5.76	265	c
129-801C	5R3 125–131	45.59	1.03	6.63	6.62	9.58	0.39	4.05	6.94	1.28	1.28	0.05	99.4	15.92	168	c
129-801C	7R3 0–5	47.04	1.97	13.82	6.40	6.46	0.15	6.18	11.16	2.79	0.44	0.10	99.5	2.95	502	c
129-801C	8R1 18–21	47.68	2.32	16.34	5.18	5.06	0.13	4.55	9.28	3.59	0.27	0.12	100.0	5.48	317	c
129-801C	8R1 65–67	46.66	2.19	15.92	7.86	2.25	0.08	2.99	10.65	3.47	0.84	0.14	100.4	7.30	269	c
129-801C	10R6 67–70	48.64	1.78	14.55	3.95	6.14	0.16	7.12	12.26	2.77	0.07	0.06	99.7	2.19	257	c
129-801C	11R2 131–136	47.19	2.11	15.15	5.19	6.64	0.16	6.00	12.01	2.59	0.10	0.17	99.6	2.29	490	c
129-801C	12R1 101–104	48.27	2.39	14.66	6.35	6.65	0.19	6.55	10.15	2.98	0.26	0.14	100.0	1.36	430	c
129-801C	12R3 57–62	48.90	2.29	13.58	4.61	7.96	0.22	6.83	11.11	2.82	0.08	0.12	99.6	1.07	623	c
185-801C	15R1 57–61	92.98	0.00250	1.10	6.27	nd	0.00761	0.102	0.246	0.0631	0.0637	0.0144	100.85	1.69	nd	d
185-801C	15R7 31–34	51.10	2.55	20.42	5.65	nd	0.149	2.02	14.26	3.82	0.529	0.266	100.76	9.07	nd	d
185-801C	17R4 15–18	42.23	0.0545	4.19	15.66	nd	0.444	4.21	27.79	0.422	4.15	0	99.15	21.08	nd	d
185-801C	19R2 24–27	70.77	0.890	4.41	12.60	nd	0.0101	9.12	1.14	1.04	0.843	0.0118	100.84	4.25	nd	d
185-801C	21R2 69–71	5.99	0.00121	0.626	3.05	nd	0.904	1.47	87.72	0.0454	0.0933	0.0140	99.93	40.73	nd	d
185-801C	25R1 10–13	48.56	2.01	13.74	13.95	nd	0.248	6.86	11.58	2.68	0.0483	0.185	99.87	0.67	nd	d
185-801C	34R1 93–96	47.93	2.41	13.80	15.68	nd	0.202	6.88	10.22	2.85	0.178	0.249	100.39	0.38	nd	d
185-801C	37R5 112–114	46.87	1.91	10.95	21.77	nd	0.131	8.88	7.19	2.43	0.433	0.207	100.77	1.66	nd	d
185-801C	40R1 24–27	42.13	1.59	10.82	11.47	nd	0.388	6.25	23.89	2.07	0.580	0.153	99.35	15.41	nd	d
185-801C	43R1 13–15	48.46	2.04	13.52	13.72	nd	0.241	6.61	11.44	2.78	0.0732	0.181	99.07	0.61	nd	d
185-801C	43R3 50–55	49.84	1.34	9.53	18.12	nd	0.191	7.58	8.22	1.94	2.24	0.107	99.09	2.43	nd	d
185-801C	44R3 23–26	47.16	2.07	14.38	13.39	nd	0.227	6.40	12.63	3.06	0.373	0.213	99.91	3.31	nd	d
Composite-801	TAB FLO	48.26	2.84	16.29	9.94	nd	0.297	5.77	8.65	3.48	3.66	0.620	99.81	7.85	nd	d
Composite-801	TAB VCL	59.95	1.43	8.45	7.14	nd	0.662	5.71	12.69	1.62	1.55	0.329	99.53	14.03	nd	d
Composite-801	TAB MIX	51.93	2.40	14.50	9.28	nd	0.406	5.70	9.88	2.90	3.24	0.548	100.79	10.08	nd	d
Composite-801	MORB 0–110 FLO	46.71	1.66	15.06	12.33	nd	0.253	5.31	15.35	2.53	0.790	0.152	100.15	9.51	nd	d
Composite-801	MORB 0–110 VCL	51.78	0.411	5.46	13.44	nd	0.322	4.43	21.66	0.717	1.389	0.0780	99.69	19.11	nd	d
Composite-801	MORB 0–110 MIX	47.85	1.32	11.97	12.72	nd	0.270	5.20	17.32	1.95	1.00	0.127	99.74	11.56	nd	d
Composite-801	MORB 110–220 FLO	48.06	2.09	14.02	13.57	nd	0.215	6.52	12.36	2.66	0.135	0.196	99.83	3.05	nd	d
Composite-801	MORB 110–220 VCL	53.11	0.969	7.16	13.31	nd	0.231	5.96	17.22	1.40	0.953	0.111	100.42	12.47	nd	d
Composite-801	MORB 110–220 MIX	49.65	1.82	12.22	13.73	nd	0.222	6.52	13.76	2.31	0.389	0.166	100.78	5.86	nd	d
Composite-801	MORB 220–420 FLO	49.70	2.04	12.70	14.63	nd	0.216	6.63	10.88	2.63	0.390	0.199	100.00	2.46	nd	d
Composite-801	MORB 220–420 VCL	51.00	1.71	10.97	15.17	nd	0.175	7.47	9.89	2.26	0.914	0.168	99.72	5.99	nd	d
Composite-801	MORB 220–420 MIX	49.67	1.94	12.38	14.56	nd	0.201	6.84	10.58	2.49	0.566	0.187	99.41	3.48	nd	d
Composite-801	SUPER	49.23	1.70	12.05	13.72	nd	0.226	6.22	13.03	2.30	0.620	0.168	99.25	6.31	nd	d
Composite-801	SED	64.61	0.191	2.52	9.73	nd	0.531	2.66	19.33	0.201	0.716	0.099	100.59	16.97	nd	d

[a] The Fe_2O_3 data from Kelley et al. (2003) represent $\sum$Fe, see note (c) below.

[b] No data.

[c] Data measured by Castillo et al. (1992) using the standard X-ray fluorescence (XRF) techniques. Note that the major element concentrations were reported as "wet" concentrations, which includes LOI concentrations (Castillo et al., 1992). All major element concentrations were converted to "dry" concentrations (excluding LOI) when plotted in Fig. 4 for comparison with the data of other samples provided by Kelley et al. (2003).

[d] Data measured by Kelley et al. (2003) using the inductivity coupled plasma mass spectrometry (ICP-MS) techniques.

containing 2–4 ppm N with low $\delta^{15}N$ values from +0.5 down to −11.4‰, including all samples from Site 1149 and Sequences IV–VIII at Site 801 (Figs. 4–6). Nitrogen concentrations and isotopic compositions of the first group are consistent with those of normal mantle, considering the low N solubility in melts (Cartigny et al., 2001; Libourel et al., 2003), and thus likely represent the composition of the mantle source emplaced at Sites 801 and 1149. The elevated N contents in the second group can be related to a sedimentary source based on the characteristics of N concentrations and isotopic compositions. Seafloor sediments are the largest ^{15}N-enriched reservoir in the deep ocean. As discussed above, a layer of seafloor sediments could have accumulated and subsequently supplied N to the later-formed "upper series" basalts via hydrothermal fluids. This possibility is supported by the presence of intercalated sediments with biostratigraphic ages as old as Middle Bathonian (167–168 Ma) in the "upper series" (Bartolini and Larson, 2001; Koppers et al., 2003). The recrystallization of the intercalated sediments demonstrates that they experienced significant hydrothermal alteration (Plank et al., 2000). The composite of the intercalated sediments from Site 801 (SED in Table 1 and Fig. 5) contains only 5.6 ppm N, significantly lower than those of the seafloor sediments just above the basaltic section (77 ppm on average, based on one radiolarite sample at 444 mbsf at Site 801B containing 78 ppm N with $\delta^{15}N$ of +3.9‰, one clay sample from 465 mbsf at Site 800A containing 37 ppm N with $\delta^{15}N$ of −0.2‰, and one silty clay sample from 422 mbsf at Site 802 containing 116 ppm N with $\delta^{15}N$ of +4.2‰; Sadofsky and Bebout, 2004), implying that significant N has been leached from the intercalated sediments, then probably redistributed into the basalts. The amounts of those previously deposited sediments are poorly constrained, but the intercalated/residual sediments are known to be a volumetrically minor component, being limited to the upper 230 m of the basement at Site 801 and making up only 2.5 vol% of the recovered cores (Plank et al., 2000).

A two-endmember mixing calculation was performed for the data in the second group, assuming the addition of sedimentary N to the MORB samples (see the upper mixing line on Fig. 6). Nitrogen concentrations and $\delta^{15}N$ values for the "fresh" MORB are represented by the data for the relatively unaltered samples from Sites 801 and 1149 in the first group (1.5 ppm and −5.6‰, respectively). Because the oldest (overlying and intercalated) sediments show a large range in $\delta^{15}N$, from −0.5‰ to +4.2‰ (Sadofsky and Bebout, 2004; this study), we used an average value of +1.8‰ to represent the isotopic composition of the sedimentary N source. Small or no isotope discrimination is considered for N transfer from sediments to AOC because most of N in the intercalated sediments has been removed. The results of our calculation show that 60–92% of the N (corresponding to 2.5–16.5 ppm) in the rocks from Sequences I and III could have been derived from the sediments (Fig. 6). If we assume that the previously deposited sediments were similar to those at the base of the sediment section at Site 801 (clay/radiolarite, see Sadofsky and Bebout, 2004), and that N in sediments was completely transferred to AOC, a simple calculation indicates that 34 m of sediments are required to achieve the current N levels in the "upper series". This thickness is consistent with the estimate of 15–45 m for the sediments accumulated during the age gap between the "lower series" and the "upper series".

The data for the third group of samples (2–4 ppm N with low $\delta^{15}N$ ranging from +0.5 to as low as −11.4‰) require a more complicated explanation. Whereas the relatively ^{15}N-enriched components from the upper part of Sequence IV and the upper part of Site 1149 (see discussion in Section 5.3) can be related to sedimentary sources, the low $\delta^{15}N$ values (−5‰ to −12‰; Fig. 5) of the other samples are not consistent with any known N sources. The lowest $\delta^{15}N$ value measured for an Earth material thus far is near −24‰ for a peridotitic diamond, a value interpreted to represent a primordial mantle signature (Cartigny et al., 1997). However, the retention of a low ("primordial") $\delta^{15}N$ in MORB source is unlikely because of the dynamic mantle processes operating beneath MOR (e.g., convection and mixing; see discussion by Cartigny et al., 1997). The basalts in the third group contain 2–4 ppm N, concentrations somewhat higher than those in the "fresh" MORB in the first group (1.5 ± 0.2 ppm; Fig. 5), seemingly representing incorporation of ^{15}N-depleted components at some point in their magmatic/crystallization or hydrothermal alteration history.

We propose a possible scenario for the incorporation of an extremely ^{15}N-depleted component into the AOC in the third group, involving abiotic reduction of the mantle-like N_2 by reaction with the H_2 produced during alteration of basaltic minerals (e.g., olivine). The product (NH_3) is then sequestrated by secondary K-bearing minerals. This process has not been observed in geological settings, but has been demonstrated to be possible under seafloor hydrothermal environments in the lab (Schoonen and Xu, 2001). If this process occured in the "lower series" at Site 801, large N-isotope fractionations of 8–11‰ (Urey, 1947) to 15–19‰ (Hanschmann, 1981) may be expected between N_2 and the NH_3 produced over the alteration temperature range of 35–95 °C (Plank et al., 2000; Alt and Teagle, 2003). Assuming a fractionation of 11‰, the resultant NH_3 from a mantle-sourced N_2 (e.g., from ascending magma and/or basaltic minerals) may have a $\delta^{15}N$ value as low as -16‰. This model requires that the amount of re-incorporated N is small relative to that of the ambient N_2. Since the N content in the "fresh" basalt is already low, the N_2 that can be liberated by alteration is too small to satisfy this requirement. Therefore, we suggest that the N was mostly sourced from outgassing of the mantle. Based on the relationship between pressure and N solubility in tholeiitic magma (Libourel et al., 2003), N content of a melt may decrease by two orders of magnitude when it ascends for 1 km. It is thus reasonable to assume that the N released from the magma is much larger than the remaining N. The latter has been detected using relatively unaltered basalts and demonstrated to be comparable to the secondary N enriched in the AOC from the "lower series", which supports a source for the extremely ^{15}N-depleted secondary N from mantle degassing. A mixing line assuming the addition of reduced N into MORB is shown in Fig. 6. This calculation

indicates that 20–60% of the N (corresponding to 0.5–2.0 ppm) in some AOC from Sites 801 and 1149 could have come from this source. Data for the composites from the "lower series" fall between the two mixing lines (but closer to the lower line; Fig. 6), implying that a small amount of sedimentary N could also have contributed to some of the AOC in this series. However, the individual samples we measured show less sedimentary-N signal than the composites, maybe because of the relatively low resolution of our analyses for the "lower series".

5.3. Comparison of N enrichment in different AOC suites

Because the majority of the secondary N in AOC is thought to be from sediments, it is possible that the intensity of incorporation of secondary N varies with time as the sediment cover progressively thickens. The samples examined in this study include the oldest oceanic basalts known on the seafloor IBM (~170 Ma) and relatively young AOC from DSDP Sites 332 and 396 in the North Atlantic (see Fig. 1a for the approximate age of each site), providing an opportunity to qualitatively consider the possible aging effect on N fixation in AOC. Compared with samples from other sites, Site 1149 samples examined in this study contain much smaller amounts of N, from 1.3 to 2.7 ppm, similar to the low-N samples from Site 801 (Table 1 and Fig. 6). Actually, the background (dark-grey) alteration is more intense at Site 1149 than at Site 801. But no high N-content samples were recovered from Site 1149. It is unknown whether a high-N zone (like Sequences I and III at Site 801) exists at Site 1149. If not, N concentrations of Site 1149 AOC, as a whole, are far lower than those for any other DSDP/ODP sites that has been examined (Table 1). The AOC samples from some much younger oceanic crusts have relatively high N concentrations (e.g., Sites 504B, 279A, 332B, and 396B). The highest N concentrations at Site 801 are comparable to the high values of much younger AOC. Overall, it appears that time/aging is not an important factor for transfer of N into AOC. Unlike the N accumulation in seafloor sediments, which increases significantly with time, particularly when the site is near the coast (Li and Bebout, 2005, 2006), the incorporation of secondary N into AOC likely occurs at early alteration stages when hydrothermal fluid activity and related mass and energy transfer are the greatest. This conclusion is consistent with observations at Site 801, where the highest N concentrations correspond to the highly recrystallized basalt sections above and beneath the Si-rich hydrothermal deposit, which indicates strong energy and mass flow (Koppers et al., 2003). In contrast with the large age or temperature range for the uptake of C (Alt and Teagle, 1999), uptake of N by old crust should be very small. This perhaps explains the low N concentrations of AOC from Site 1149. At early alteration stages of this section, the lack of a sedimentary N source restricted large enrichment of N in the basalts although the alteration (dark-grey type) they experienced was intense. The basalts hence retained the low N concentrations because, although more N became available with off-axis sediment accumulation, the energy in the topmost basalts close to the sediments was reduced and unable to activate fluid to transfer N from the sediments to the basalts.

5.4. Subducting N budget in oceanic crust

This study enables us to make an initial attempt at characterizing in detail the N inventory of the subducting oceanic crust at the reference site near the Mariana trench. We used a method similar to those for the calculation of C and N inventories of the seafloor sediments at "Subduction Factory" reference sites (Sadofsky and Bebout, 2004; Li and Bebout, 2005) to estimate the subducting N budget in oceanic crust. The N inventory at Site 801 was calculated on an individual-sample basis. Nitrogen concentration and isotopic composition of each sample are assumed to represent the mean values of the AOC section between itself and the next shallower sample, providing a higher resolution than would be possible using the AOC composites. This calculation indicates that the upper 470 m basement at Site 801 (section that was recovered by ODP Legs 129 and 185) carries an annual N flux of 8×10^5 g/km, with mean $\delta^{15}N$ of $-2.9‰$, into the IBM margin. However, little is known regarding the N geochemistry for the remainder of the crustal section, which is mostly composed of dikes and gabbros. If we assume an average N concentration of 1.5 ppm, with mean $\delta^{15}N$ of $-5.6‰$ (as discussed above), for the remaining 6.5 km of crust (assuming an average oceanic crustal thickness of 7 km; White et al., 1992), the entire oceanic crust section would annually contribute 5.1×10^6 g/km N with mean $\delta^{15}N$ of $-5.2‰$ to the Mariana trench. This AOC N subduction flux is twice as large as the sedimentary annual N flux of 2.5×10^6 g/km into the same margin (Sadofsky and Bebout, 2004). These data indicate that AOC is a major carrier of subducting N, despite the relatively low concentrations, because of the large volumes of oceanic crust being subducted. If the contribution of sediments (Sadofsky and Bebout, 2004) is incorporated, the full oceanic crust + sediment section introduces 7.6×10^6 g/km N, with $\delta^{15}N$ of $-1.8‰$, into the Mariana trench.

Subduction mass-balance based on comparisons of N input in trench and N output based on study of volcanic gases must consider a daunting set of uncertainties including the unknown magnitudes of N incorporation into volcanic and plutonic rocks in the arc (i.e., not degassed), spatial and temporal variations of both input and output within individual arc-trench segments, and N loss due to devolatilization in the forearc. Because the magnitude of these uncertainties is large, any estimates of subduction recycling efficiency must be regarded as semi-quantitative at best. The impact of subduction on the mantle N isotopic signature depends on the extent of metamorphic devolatilization and resulting increase in the $\delta^{15}N$ values of the residual ammonium. The extent of N loss during metamorphic devolatilization is probably strongly related to the thermal evolution of individual subduction zones, with more efficient delivery of N into the deep mantle occurring in relatively "cool" margins into which old, cool oceanic lithosphere is being subducted rapidly (Bebout and Fogel, 1992; Bebout et al., 1999; Busigny et al., 2003; Bebout, in press). In subducting slabs, most of the N in AOC subducted to beyond the shallow forearc is

likely structurally bound in potassium-bearing minerals (particularly the micas), which should be more resistant to subduction-related metamorphic degassing than the organic N in seafloor sediments. Some fraction of the sedimentary N may be easily lost during the transfer of organic N into phyllosilicates during diagenesis and low-T metamorphism. Nevertheless, many recent studies of arc element and isotope geochemistry have invoked additions of sediment melts (in particular to explain Th and ^{10}Be enrichments in arc lavas; see Elliott, 2003), and it is possible that, beneath arcs, N release is governed by some combination of metamorphic devolatilization and partial melting. A transition in the physicochemical characteristics of slab-derived fluids across arcs, from dominantly hydrous fluid to dominantly silicate melt (or supercritical liquid; see Hermann et al., 2006), could influence the efficiency of N release and the N isotopic composition of the "fluid" released from subducting materials. In the case that the subduction/input N flux into the trench is much larger than the degassing/output N fluxes at arcs (e.g., at the Central American convergent margin, see Li and Bebout, 2005; no output data available so far for IBM margin), if N loss during early metamorphic devolatilization in the subduction zone is relatively small, subduction results in net addition of N to the deeper mantle. However, because the subducting oceanic crust has an average δ^{15}N similar to that of the mantle, if there is no significant isotopic shift related to N loss in the shallow forearc, the recycled N_2 in the arc may be isotopically indistinguishable from the N_2 from the mantle, and the deep subduction of oceanic crust may not impact the δ^{15}N of the mantle. However, the deep subduction of ^{15}N-enriched sedimentary N may potentially affect the mantle δ^{15}N, perhaps explaining the high δ^{15}N values of the carbonatite from Kola Peninsula reported by Dauphas and Marty (1999).

6. CONCLUSIONS

Altered oceanic crust shows significant enrichment in N compared with concentrations in fresh MORB. The secondary N in AOC, as ammonium structurally bound in silicates, is added by circulating hydrothermal fluids. Seafloor sediment is the likely source of most of the enriched N in the AOC from the "upper series" at Site 801, whereas a reduced N form evolved from mantle-like N_2 and characterized by extremely negative δ^{15}N could be responsible for the N enrichment in most of the rocks from the "lower series", where sedimentary N was not available during alteration. The incorporation of the secondary N probably occurs in the early alteration stages of AOC. Taking into account the additions of N by seafloor alteration, we estimate that the basement section near the Mariana margin is annually subducting 5.1×10^6 g/km N into the trench. This rate for N subduction in oceanic crust is twice as large as that of sedimentary N input into the same margin. Overall, the subducting slab in the Mariana margin (the sediment and complete oceanic crust section) contributes an annual N flux of 7.6×10^6 g/km with δ^{15}N of $-1.8‰$. Metamorphic devolatilization, and potentially also partial melting, dictates the amount of ^{15}N-enriched N that is conveyed into the mantle beyond subarc regions, and it remains unclear whether the volcanic arc preferentially returns the sedimentary N component in this subducting section (see the discussion by Elkins et al., 2006). Further study of N output in the IBM volcanic arc is required for a better understanding of N cycling across the IBM margin.

ACKNOWLEDGMENTS

This research utilized samples and data provided by the Ocean Drilling Program (ODP), which is sponsored by the United States National Science Foundation (NSF) and participating countries under management of Joint Oceanographic Institutions (JOI), Inc. Funding for this study was provided by the JOI-USSSP and NSF (EAR-0409008) to GEB. We thank Leg 185 co-chief scientists T. Plank and J. Ludden and the Scientific Party of Leg 185 for their support of our shore-based research. We also thank K. Kelley and P. Castillo for providing samples from Sites 801 and 1149 and T. Elliott for providing the other samples. This manuscript was improved by constructive reviews by J. Alt, P. Cartigny, T. Fischer, and S. Sadofsky. We also thank J. Alt for editorial handling of this paper.

REFERENCES

Ader M., Cartigny P., Boudou J.-P., Oh J.-H., Petit E., and Javoy M. (2006) Nitrogen isotopic evolution of carbonaceous matter during metamorphism: methodology and preliminary results. *Chem. Geol.* **232**, 152–169.

Alt J. C. (2003) Stable isotopic composition of upper oceanic crust formed at a fast spreading ridge, ODP Site 801. *Geochem. Geophys. Geosyst.* **4**, 8908. doi:10.1029/2002GC000400.

Alt J. C., and Teagle D. A. H. (1999) The uptake of carbon during alteration of ocean crust. *Geochim. Cosmochim. Acta* **63**, 1527–1535.

Alt J. C., and Teagle D. A. H. (2003) Hydrothermal alteration of upper oceanic crust formed at a fast-spreading ridge: mineral, chemical, and isotopic evidence from ODP Site 801. *Chem. Geol.* **201**, 191–211.

Alt J. C., Honnorez J., Laverne C., and Emmermann R. (1986) Hydrothermal alteration of a 1 km section through the upper oceanic crust, Deep Sea Drilling Project Hole 504B: the mineralogy, chemistry, and evolution of seawater–basalt interactions. *J. Geophys. Res.* **91**, 10,309–10, 355.

Alt J. C., France-Lanord C., Floyd P. A., Castillo P., and Galy A. (1992). Low-temperature hydrothermal alteration of Jurassic ocean crust, Site 801. In *Proc. Ocean. Drill. Prog., Sci. Results.*, vol. 129 (eds. R. L. Larson, Y. Lancelot, et al.). College Station, TX (Ocean Drilling Program), pp. 415–427.

Alt J. C., Teagle D. A. H., Laverne C., Vanko D. A., Bach W., Honnorez J., Becker K., Ayadi M., and Pezard P. A. (1996). Ridge flank alteration of upper ocean crust in the Eastern Pacific: synthesis of results for volcanic rocks of Holes 504B and 896A. In *Proc. Ocean. Drill. Prog., Sci. Results.*, vol. 148 (eds. J. C. Alt, H. Kinoshita, L. B. Stokking, and P. J. Michael). College Station, TX (Ocean Drilling Program), pp. 435–450.

Bach W., and Edwards K. J. (2003) Iron and sulfide oxidation within the basaltic ocean crust: implications for chemolithoautotrophic microbial biomass production. *Geochim. Cosmochim. Acta* **67**, 3871–3887.

Bartolini A., and Larson R. (2001) Pacific microplate and the Pangea supercontinent in the Early to Middle Jurassic. *Geology* **29**, 735–738.

Bebout G. E. (1995) The impact of subduction-zone metamorphism on mantle-ocean chemical cycling. *Chem. Geol.* **126**, 191–218.

Bebout G. E. (in press) Chemical and isotopic cycling in subduction zones. Treatise on Geochemistry. Elsevier.

Bebout G. E., and Fogel M. L. (1992) Nitrogen-isotope compositions of metasedimentary rocks in the Catalina Schist, California: implications for metamorphic devolatilization history. *Geochim. Cosmochim. Acta* **56**, 2839–2849.

Bebout G. E., Ryan J. G., Leeman W. P., and Bebout A. E. (1999) Fractionation of trace elements by subduction-zone metamorphism—effects of convergent-margin thermal evolution. *Earth Planet. Sci. Lett.* **171**, 63–81.

Bebout G. E., Idleman B. D., Li L., and Hilkert A. (2004) High-precision isotopic analysis of nanomole quantities of silicate nitrogen. Extended abstract in *Water–Rock Interaction.*, vol. 1 (eds. R. B. Wanty, R. R. Seal III, and A. A. Balkema). Brookfield, Vermont.

Bebout G. E., Idleman B. D., Li L., and Hilkert A. (2007) Isotope-ratio-monitoring gas chromatography methods for high-precision isotopic analysis of nanomole quantities of silicate nitrogen. *Chem. Geol.*, doi:10.1016/j.chemgeo.2007.01.006.

Bos A., Duit W., van der Eerden A. M. J., and Jansen J. B. H. (1988) Nitrogen storage in biotite: an experimental study of the ammonium and potassium partitioning between 1 M-phlogopite and vapor at 2 kb. *Geochim. Cosmochim. Acta* **52**, 1275–1283.

Boyd S. R., Pillinger C. T., Milledge H. J., Mendelssohn M. J., and Seal M. (1992) C and N isotopic composition and the infrared absorption spectra of coated diamonds: evidence for the regional uniformity of CO_2–H_2O rich fluid in lithospheric mantle. *Earth Planet. Sci. Lett.* **109**, 633–644.

Brandes J. A., Devol A. H., Yoshinari T., Jayakumar D. A., and Naqvi S. W. A. (1998) Isotopic composition of nitrate in the central Arabian Sea and eastern tropical North Pacific: a tracer for mixing and nitrogen cycles. *Limnol. Oceanogr.* **43**, 1680–1689.

Busigny V., Laverne C., and Bonifacie M. (2005a) Nitrogen content and isotopic composition of oceanic crust at a superfast spreading ridge: a profile in altered basalts from ODP Site 1256, Leg 206. *Geochem. Geophys. Geosyst.* **6**, Q12O01. doi:10.1029/2005GC001020.

Busigny V., Ader M., and Cartigny P. (2005b) Quantification and isotopic analysis of nitrogen in rocks at the ppm level using sealed-tube combustion technique: a prelude to the study of altered oceanic crust. *Chem. Geol.* **223**, 249–259.

Busigny V., Cartigny P., Philippot P., Ader M., and Javoy M. (2003) Massive recycling of nitrogen and other fluid-mobile elements (K, Rb, Cs, H) in a cold slab environment: evidence from HP to UHP oceanic metasediments of the Schistes Lustres nappe (western Alps, Europe). *Earth Planet. Sci. Lett.* **215**, 27–42.

Cartigny P., Boyd S. R., Harris J. W., and Javoy M. (1997) Nitrogen isotopes in peridotitic diamonds from Fuxian, China: the mantle signature. *Terra Nova* **9**, 175–179.

Cartigny P., Jendrzejewski N., Pineau F., Petit E., and Javoy M. (2001) Volatile (C, N, Ar) variability in MORB and the respective roles of mantle source heterogeneity and degassing: the case of the Southwest Indian Ridge. *Earth Planet. Sci. Lett.* **194**, 241–257.

Cartigny P., Harris J. W., Taylor A., Davies R., and Javoy M. (2003) On the possibility of a kinetic fractionation of nitrogen stable isotopes during natural diamond growth. *Geochim. Cosmochim. Acta* **67**, 1571–1576.

Castillo P. R., Floyd P. A., France-Lanord C., and Alt J. C. (1992) Data report: summary of geochemical data for Leg 129 igneous rocks. In *Proc. Ocean. Drill. Prog., Sci. Results.*, vol. 129 (eds. Larson, R.L., Lancelot, Y. et al.). College Station, TX (Ocean Drilling Program), pp. 653–670.

Cline J. D., and Kaplan I. R. (1975) Isotopic fractionation of dissolved nitrate during denitrification in the eastern tropical North Pacific Ocean. *Mar. Chem.* **3**, 271–299.

Dauphas N., and Marty B. (1999) Heavy nitrogen in carbonatites of the Kola Peninsula: a possible signature of the deep mantle. *Science* **286**, 2488–2490.

Elkins L. J., Fischer T. P., Hilton D. R., Sharp Z. D., Mcknight S., and Walker J. (2006) Tracing nitrogen in volcanic and geothermal volatiles from the Nicaraguan volcanic front. *Geochim. Cosmochim. Acta* **70**, 5215–5235.

Elliott T. (2003) Tracers of the slab. In *Inside the Subduction Factory. Amer. Geophys. Un. Geophys. Monogr.*, vol. 138 (ed. J. Eiler). Amer. Geophys. Union, Washington DC, pp. 23–45.

Exley R. A., Boyd S. R., Mattey D. P., and Pillinger C. T. (1987) Nitrogen isotope geochemistry of basaltic glasses: implications for mantle degassing and structure? *Earth Planet. Sci. Lett.* **81**, 163–174.

Fischer T. P., Hilton D. R., Zimmer M. M., Shaw A. M., Sharp Z. D., and Walker J. A. (2002) Subduction and recycling of nitrogen along the Central American margin. *Science* **297**, 1154–1157.

Fischer T. P., Takataha N., Sano Y., Sumino H., and Hilton D. R. (2005) Nitrogen isotopes of the mantle: Insights from mineral separates. *Geophys. Res. Lett.* **32**, L11305. doi:10.1029/2005GL022792.

Fisk M. R., Staudigel H., Smith D. C., and Haveman S. (1999) Evidence of microbial activity in the oldest oceanic crust. *Eos Trans. Am. Geophys. Union* **80**, Fall Meet. Suppl. # B42B-04 (abstr.).

Floyd P. A., Winchester J. A., and Castillo P. R. (1992) Geochemistry and petrography of Cretaceous sills and lava flows, Sites 800 and 802. In *Proc. Ocean. Drill. Prog., Sci. Results.*, vol. 129 (eds. R. L. Larson, Y. Lancelot et al.). College Station, TX (Ocean Drilling Program), pp. 345–359.

Hanschmann G. (1981) Berechnung von isotopieeffekten auf quantenchemischer grundlage am beispiel stickstoffhaltiger molecule. *Zfi-Mitteilungen* **41**, 19–31.

Hart S. R., Erlank A. J., and Kable E. J. D. (1974) Sea floor basalt alteration: some chemical and Sr isotopic effects. *Contrib. Mineral. Petrol.* **44**, 219–230.

Hermann J., Spandler C., Hack A., and Korsakov A. V. (2006) Aqueous fluids and hydrous melts in high-pressure and ultra-high pressure rocks: implications for element transfer in subduction zones. *Lithos* **92**, 399–417.

Hilton D. R., Fischer T. P., and Marty B. (2002) Noble gases and volatile recycling at subduction zones. In *Noble Gases in Geochemistry and Cosmochemistry, Rev. Mineral. Geochem.*, vol. 47 (eds. D. Porcelli, C. Ballentine, and R. Weiler). Mineral. Soc. Amer., Washingon DC, pp. 319–370.

Honma H., and Itihara Y. (1981) Distribution of ammonium in minerals of metamorphic and granitic rocks. *Geochim. Cosmochim. Acta* **45**, 983–988.

Jarrard R. D. (2003) Subduction fluxes of water, carbon dioxide, chlorine, and potassium. *Geochem. Geophys. Geosyst.* **4**, 8905. doi:10.1029/2002GC00039.

Javoy M. (1998) The birth of the Earth's atmosphere: the behavior and the fate of its major elements. *Chem. Geol.* **147**, 11–25.

Javoy M., and Pineau F. (1991) The volatile record of a "popping" rock from the Mid-Atlantic Ridge at 14°N: chemical and isotopic composition of gas trapped in the vesicles. *Earth Planet. Sci. Lett.* **107**, 598–611.

Javoy M., Pineau F., and Demaiffe D. (1984) Nitrogen and carbon isotopic composition in the diamonds of Mbuji Mayi (Zaire). *Earth Planet. Sci. Lett.* **68**, 399–412.

Kelley K. A., Plank T., Ludden J., and Staudigel H. (2003) Composition of altered oceanic crust at ODP Sites 801 and 1149. *Geochem. Geophys. Geosyst.* **4**, 8910. doi:10.1029/2002GC000435.

Koppers A. A. P., Staudigel H., and Duncan R. A. (2003) High-resolution $^{40}Ar/^{39}Ar$ dating of the oldest oceanic basement basalts in the western Pacific basin. *Geochem. Geophys. Geosyst.* **4**, 8914. doi:10.1029/2003GC000574.

Lancelot Y., Larson R., Fisher A. T., and Scientific Party (1990) In *Proc. Ocean. Drill. Prog., Init. Repts.*, vol. 129, College Station, TX (Ocean Drilling Program).

Li L., and Bebout G. E. (2005) Carbon and nitrogen geochemistry of sediments in the Central American convergent margin: insights regarding subduction input fluxes, diagenesis, and paleoproductivity. *J. Geophys. Res.* **110**, B11202. doi:10.1029/2004JB003276.

Li L., and Bebout G.E. (2006) Carbon and nitrogen geochemistry of wedge sediments at ODP Site 1040: evidence for sediment sources, diagenetic history, and fluid mobility. In *Proc. Ocean. Drill. Prog., Sci. Results.*, vol. 205 (eds. J. D. Morris, H. W. Villinger, and A. Klaus), pp. 1–38 (http://www-odp.tamu.edu/publications/205_SR/VOLUME/CHAPTERS/214.PDF).

Libourel G., Marty B., and Humbert F. (2003) Nitrogen solubility in basaltic melt. Part I. Effect of oxygen fugacity. *Geochim. Cosmochim. Acta* **67**, 4123–4135.

Lilley M. D., Butterfield D. A., Olson E. J., Lupton J. E., Macko S. A., and McDuff R. E. (1993) Anomalous CH_4 and NH_4^+ concentrations at an unsedimented mid-ocean-ridge hydrothermal system. *Nature* **364**, 45–47.

Marty B. (1995) Nitrogen content of the mantle inferred from N_2-Ar correlation in oceanic basalts. *Nature* **377**, 326–329.

Marty B., and Humbert F. (1997) Nitrogen and argon isotopes in oceanic basalts. *Earth Planet. Sci. Lett.* **152**, 101–112.

Marty B., and Zimmermann L. (1999) Volatiles (He, C, N, Ar) in mid-ocean ridge basalts: assessment of shallow-level fractionation and characterization of source composition. *Geochim. Cosmchim. Acta* **63**, 3619–3633.

Mottl M. J., and Holland H. D. (1978) Chemical exchange during hydrothermal alteration of basalt by seawater - I. Experimental results for major and minor components of seawater. *Geochim. Cosmochim. Acta* **42**, 1103–1115.

Nishio Y., Ishii T., Gamo T., and Sano Y. (1999) Volatile element isotopic systematics of the Rodrigues Triple Junction Indian Ocean MORB: implications for mantle heterogeneity. *Earth Planet. Sci. Lett.* **170**, 241–253.

Philippot P., Agrinier P., and Scambelluri M. (1998) Chlorine recycling during subduction of altered oceanic crust. *Earth Planet. Sci. Lett.* **161**, 33–44.

Plank T., Ludden J. N., Escutia C., and Scientific Party (2000) In *Proc. Ocean. Drill. Prog., Init. Repts.*, vol. 185 (http://www-odp.tamu.edu/publications/185_IR/185ir.htm).

Pockalny R. A., and Larson R. L. (2003) Implications for crustal accretion at fast spreading ridges from observations in Jurassic oceanic crust in the western Pacific. *Geochem. Geophys. Geosyst.* **4**, 8903. doi:10.1029/2001GC000274.

Pringle M. S. (1992) Radiometric ages of basaltic basement recovered at Sites 800, 801, and 802, Leg 129, Western Pacific Ocean. In *Proc. Ocean. Drill. Prog., Sci. Results.*, vol. 129 (eds. R. L. Larson, Y. Lancelot et al.). College Station, TX (Ocean Drilling Program), pp. 389–404.

Proskurowski G., Lilley M. D., and Brown T. A. (2004) Isotopic evidence of magmatism and seawater bicarbonate removal at the Endeavour hydrothermal system. *Earth Planet. Sci. Lett.* **225**, 53–61.

Sadofsky S. J., and Bebout G. E. (2004) Nitrogen geochemistry of subducting sediments: new results from the Izu-Bonin-Mariana margin and insights regarding global nitrogen subduction. *Geochem. Geophys. Geosyst.* **5**, Q03l15. doi:10.1029/2003GC000543.

Sano Y., Takahata N., Nishio Y., and Marty B. (1998) Nitrogen recycling in subduction zones. *Geophys. Res. Lett.* **25**, 2289–2292.

Sano Y., Takahata N., Nishio Y., Fischer T., and Williams S. N. (2001) Volcanic flux of nitrogen from the Earth. *Chem. Geol.* **171**, 263–271.

Schoonen M. A. A., and Xu Y. (2001) Nitrogen reduction under hydrothermal vent conditions: implications for the prebiotic synthesis of C–H–O–N compounds. *Astrobiology* **1**, 133–142.

Scholl D. W. and von Huene R. (in press) Crustal recycling at modern subduction zones applied to the past—issues of growth and preservation of continental basement, mantle geochemistry, and supercontinent reconstruction. *Geol. Soc. Amer. Spec. Paper*.

Schroeder P. A., and McLain A. A. (1998) Illite-smectites and the influence of burial diagenesis on the geochemical cycling of nitrogen. *Clay Mineral.* **33**, 539–546.

Snyder G., Poreda R., Fehn U., and Hunt A. (2003) Sources of nitrogen and methane in Central American geothermal settings: nobel gas and ^{129}I evidence for crustal and magmatic volatile components. *Geochem. Geophys. Geosyst.* **4**, 9001. doi:10.1029/2002GC000363.

Staudigel H., Davies G. R., Hart S. R., Marchant K. M., and Smith B. M. (1995) Large scale isotopic Sr, Nd and O isotopic anatomy of altered oceanic crust: DSDP/ODP Site 417/418. *Earth Planet. Sci. Lett.* **130**, 169–185.

Staudigel H., Plank T., White W., and Schmincke H. U. (1996) Geochemical fluxes during seafloor alteration of the basaltic upper oceanic crust: DSDP Sites 417 and 418. In *Subduction: Top to Bottom, Am. Geophys. Union, Geophys. Monogr.*, vol. 96 (eds. G. E. Bebout, D. W. Scholl, S. H. Kirby, and J. P. Platt). Amer. Geophys. Union, Washington DC, pp. 19–38.

Staudigel H., Furnes H., Banerjee N. R., Dilek Y., and Muelenbachs K. (2006) Microbes and volcanoes: a tale from the oceans, ophiolites, and greenstone belts. *GSA Today* **16** (10), 4–10. doi:10.1130/GSAT01610A.1.

Stevens T. O., and McKinley J. P. (2000) Abiotic controls on H_2 production from basalt-water reactions and implications for aquifer biogeochemistry. *Environ. Sci. Technol.* **34**, 826–831.

Tolstikhin I. N., and Marty B. (1998) The evolution of terrestrial volatiles: a view from helium, neon, argon and nitrogen isotope modeling. *Chem. Geol.* **147**, 27–52.

Urey H. C. (1947) The thermodynamic properties of isotopic substances. *J. Chem. Soc. (London)*, 562–581. doi:10.1039/JR9470000562.

White R. S., McKenzie D., and O'Nions R. K. (1992) Oceanic crustal thickness from seismic measurements and rare earth element inversions. *J. Geophys. Res.* **97**, 19,683–19,715.

Williams L. B., Ferrell, Jr., R. E., Hutcheon I., Bakel A. J., Walsh M. M., and Krouse H. R. (1995) Nitrogen isotope geochemistry of organic matter and minerals during diagenesis and hydrocarbon migration. *Geochim. Cosmochim. Acta* **59**, 765–779.

Wilson D. S., Teagle D. A. H., Acton G. D. et al. (2003) In *Proc. ODP, Init. Repts.*, vol. 206 (http://www-odp.tamu.edu/publications/206_IR/206ir.htm).

Yamamoto T., and Nakahira M. (1966) Ammonium ions in sericites. *Am. Mineral.* **51**, 1775–1786.

Zhang Y., and Zindler A. (1993) Distribution and evolution of carbon and nitrogen in Earth. *Earth Planet. Sci. Lett.* **117**, 331–345.

Zimmer M. M., Fischer T. P., Hilton D. R., Alvarado G. E., Sharp Z. D., and Walker J. A. (2004) Nitrogen systematics and gas fluxes of subduction zones: insights from Costa Rica arc volatiles. *Geochem. Geophys. Geosyst.* **5**, Q15J11. doi:10.1029/2003GC000651.

Associate editor: Jeffrey C. Alt